



Emergence of strain induced two dimensional metallic state in ReS₂



P.C. Sreeparvathy^a, V. Kanchana^{a,*}, P. Anees^b, G. Vaitheeswaran^{c,d}

^a Department of Physics, Indian Institute of Technology Hyderabad, Kandi, 502285 Sangareddy, Telangana, India

^b Materials Physics Division, Indira Gandhi Centre for Atomic Research, Kalpakkam 603102, India

^c Advanced Centre of Research in High Energy Materials (ACRHEM), University of Hyderabad, Prof. C. R. Rao Road, Gachibowli, Hyderabad 500046, Telangana, India

^d School of Physics, University of Hyderabad, Prof. C. R. Rao Road, Gachibowli, Hyderabad 500046, Telangana, India

ARTICLE INFO

Keywords:

Electronic structure
Thermoelectric properties
Strain

ABSTRACT

We present a highly versatile system ReS₂, which transforms from a semiconductor to a two dimensional metal under uni-axial compressive strain along 'a' direction in both bulk and monolayer. The 2D nature is realised from highly flat Fermi surfaces and anisotropic transport properties. Moreover the layer independent electronic structure properties are revisited and thermoelectric properties of ReS₂ in bulk, monolayer and bilayer forms reveal the competing thermoelectric (TE) coefficients in each form. The in-plane power-factor shows an enhancement over 'c'-axis value as a function of strain, which is almost two orders of magnitude. In addition, strain induced tunable in-plane anisotropy of almost one order has been observed in both bulk and monolayer ReS₂ (around 20%), which further open up the possibility of TE application as nanowires. Our analysis unveils a wide range of application for ReS₂ in the field of thermoelectrics as bulk and thin films for a large temperature range. The magnitude of TE coefficients are comparable with other well established transition metal dichalcogenides.

1. Introduction

The realization of two dimensional nature in transition metal dichalcogenide (TMD) has elevated the research pertaining to TMD to the next level [1–6]. The isolated 2D transition metal dichalcogenide layers have been competing with the two dimensional material like graphene which has several importance in the current technologies. The strong intra layer bonding and weak inter layer bonding in the layered materials is quite interesting, leading to the usage of these materials in the bulk and layered forms [7–9]. ReS₂ is one of the transition metal dichalcogenides which stands out with very peculiar properties, and has drawn adequate attention in the recent past. Unlike the other layered transition metal dichalcogenides, ReS₂ crystallizes in a triclinic space group. Recent study reveals that the interaction between layers in ReS₂ is negligible implying that the monolayer of ReS₂ might have similar electronic properties as that of bulk, enabling ReS₂ to be the highlight in the last decade [10]. Pressure and strain are the robust tools which can modify the structure and electronic properties of materials, and transition metal dichalcogenides showed considerable response to strain and pressure [11–13], leading to metallization at high pressure, direct to indirect band gap transitions etc. Optical and electronic properties are also explored for both bulk and

layered ReS₂ [14], and this compound has found application in field effect transistors [15,16]. The inherent structural anisotropy of ReS₂ has further shown an influential response towards pressure and strain, resulting in tuning of in-plane, and through plane anisotropy in several physical properties like resistivity, charge mobility etc, and significant number of studies are dedicated to understand this especially for monolayer ReS₂ [17–21]. Though plethora literatures are available exploring ReS₂ in several directions, studies addressing the physical properties and its anisotropic behaviour along different crystallographic directions of ReS₂ (where the out of plane component does not represent the other crystallographic direction as the symmetry is triclinic) are less investigated, and one of the earlier study has reported the anisotropy in resistivity along 'b' and 'c' axes experimentally, and it is worthy to analyse these properties in detail. In addition, studies related to pressure induced structural transitions and metallization are also reported [22]. Here we would like to explore the effect of uni-axial strain on bulk and few layers of ReS₂ using first principles calculations. The well studied TMD like MoS₂ is already explored for straintronic applications [23], and we expect ReS₂ to be yet another perspective compound. As discussed earlier, TMD materials have wide spread applications, and one of the significant application is thermoelectric power generation. Thermoelectric materials can convert waste heat

* Corresponding author.

E-mail address: kanchana@iith.ac.in (V. Kanchana).

Table 1
Calculated ground state properties of bulk and monolayer ReS₂.

ReS ₂	a(Å)	b(Å)	c(Å)	Volume(Å ³)
Bulk(with vdW) _{present}	6.31	6.53	6.46	218.76
Bulk (without vdW) _{present}	6.41	6.52	7.00	242.5
Bulk _{exp} [38]	6.45	6.39	6.4	218.68
Bulk _{exp} [56]	6.417	5.510	5.461	219.32
Mono – layer _{present}	6.31	6.49	21.34	765.3

into electricity and waste heat generation is one of the grand challenges in the present world. In this scenario exploring novel materials for thermoelectric conversion is worth investigating. The capability of a TE material is quantified using a dimensionless quantity called figure of merit (ZT). $ZT = S^2\sigma T/\kappa$, where S , σ , κ , and T are the thermopower, the electrical conductivity, the thermal conductivity, and the absolute temperature, respectively. κ includes both the electronic, κ_e , and the lattice contributions, κ_l , i.e., $\kappa = \kappa_e + \kappa_l$. The rest of the manuscript is organized as follows, Section 2 describes the computational methods used for the present work, Section 3 describes the structure, electronic and transport properties at ambient and strained states, followed by conclusions.

2. Computational details

We have used the experimental structure parameters for ReS₂ and performed a complete geometry optimization and phonon dispersion

using VASP [24,25]. Since ReS₂ possess a layered structure, we have included van der Waals correction using Tkatchenko -Scheffler method [26] (see Table 1). Further electronic structure properties like band structure, Fermi surface etc were calculated using full potential linearised augmented plane wave (FP-LAPW) method implemented in WIEN2k package [27,28]. Different layered structures of ReS₂ were cleaved from the bulk materials, and vacuum convergence are performed for each layered structure with a k-mesh of $10 \times 10 \times 9$ for bulk and $12 \times 12 \times 3$ for layers. The applied vacuum for monolayer and bilayer structure is around 15 angstroms. We have performed super cell calculation to ensure that the properties remain unchanged, and, have continued with 4 Re and 8 S atom unit cell only. Presence of heavy elements in the investigated compounds warrants the inclusion of spin orbit coupling in our calculations. Transport coefficients such as thermopower (S in μVK^{-1}) and electrical conductivity scaled by relaxation time (σ/τ in $\Omega^{-1}\text{m}^{-1}\text{s}^{-1}$) were calculated using BoltzTraP code [29] with a dense k-mesh of the order of $32 \times 36 \times 25$ k-points resulting 14402 k-points in irreducible Brillouin zone. Two major assumptions are incorporated in BoltzTraP code, one is rigid band approximation (RBA) [30–32] and the other is constant scattering time approximation (CSTA), and appreciable number of thermoelectric materials are successfully predicted using the same [33–37].

3. Results and discussions

3.1. Structure and stability of Investigated compound

ReS₂ crystallizes in distorted triclinic symmetry [38], which is

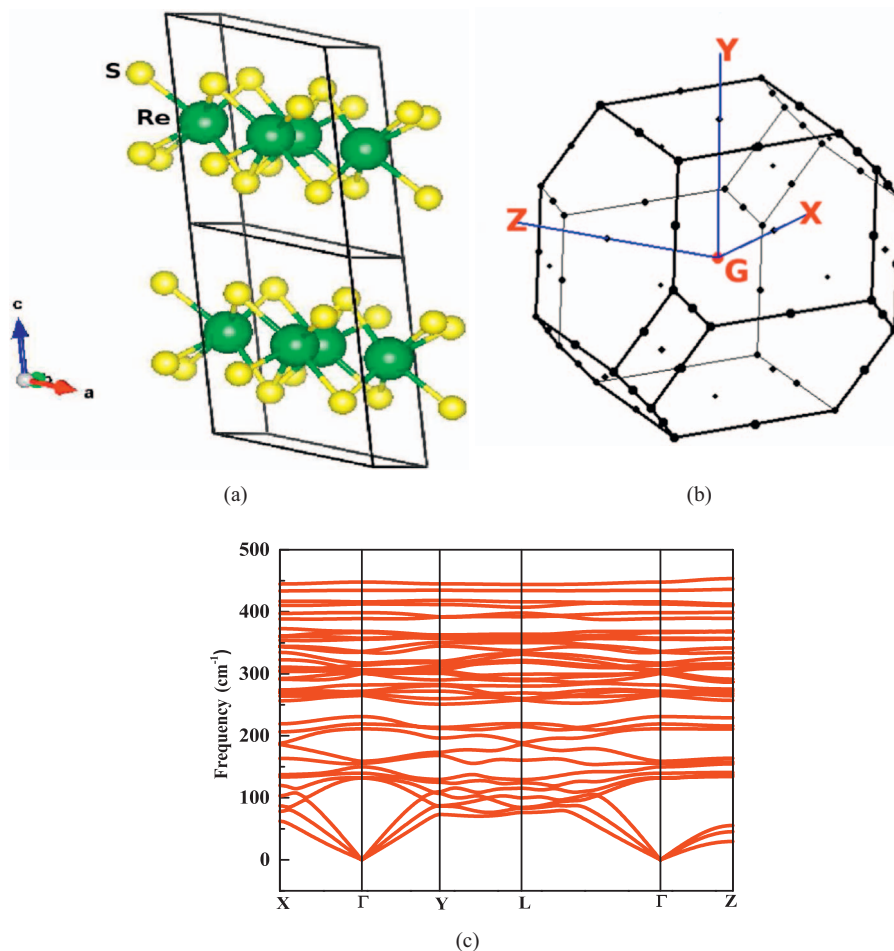


Fig. 1. (a) Crystal structure (green color represent 'Re' and yellow color represent 'S') (b) Phonon dispersion spectra of bulk ReS₂ in triclinic structure. (For interpretation of the references to color in this figure legend, the reader is referred to the web version of this article.)

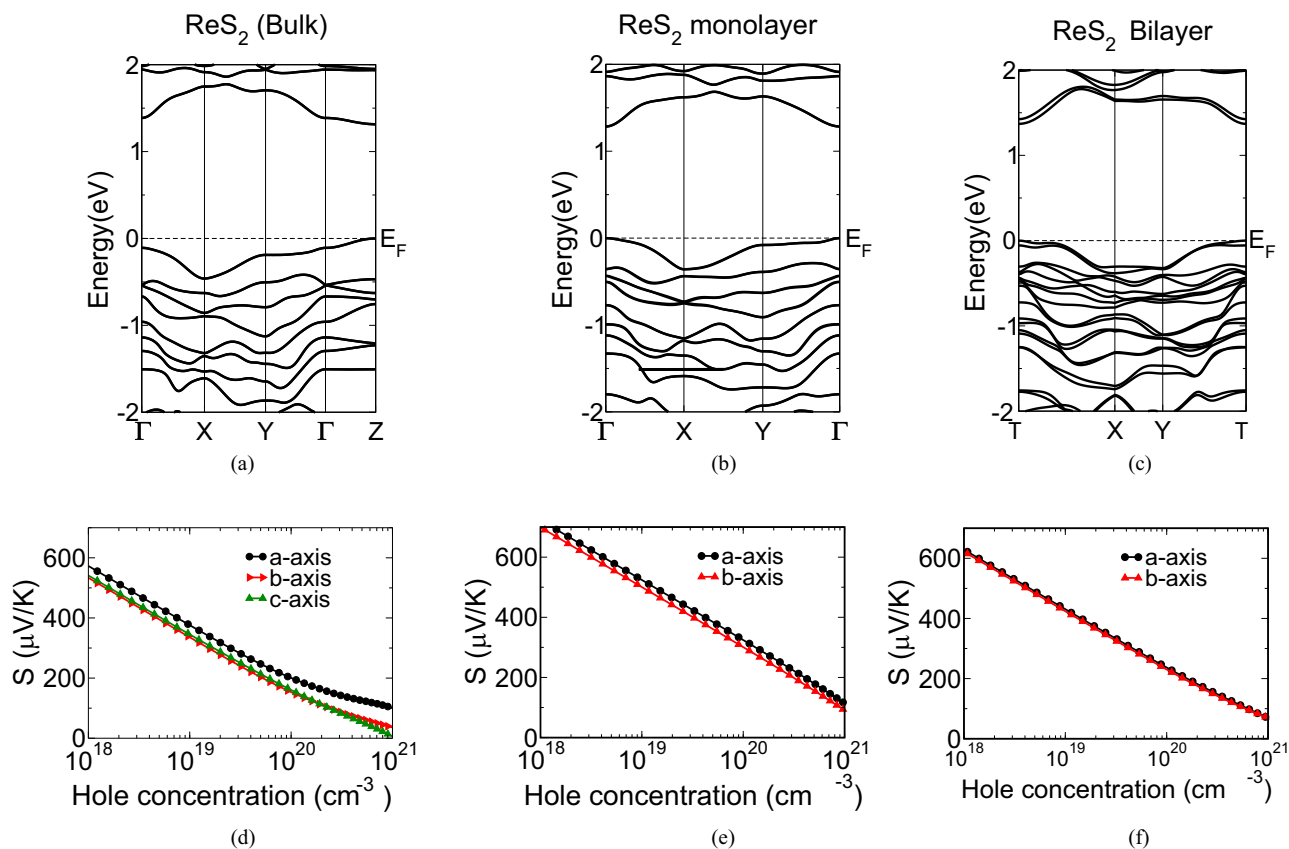


Fig. 2. (a) Band structure of bulk ReS₂ (which shows small 2D nature), (b) for monolayer (c) for Bilayer, Thermopower of (d) bulk, (e) monolayer and (f) bilayer (which indicate the layer independent TE property).

exceptional in TMD. One of the recent study has reported a structural transition of the compound at around 0.1 GPa, and named the ambient one as distorted 3R and the transformed structure as distorted 1T structure [22]. From our analysis we have observed the energy difference between these two structures to be negligibly small and one can conclude these to be competing structures, and in this scenario, we have progressed our calculation with 3R structure which is experimentally reported. The details of the experimental crystal structure, together with present optimized values are given in Table 1. The weak interlayer bonding of this compound is well known [10] and we have optimized the structure by adding the van der Waals correction. The cleaved monolayer and bilayer structure also preserve triclinic symmetry. The two 'Re' chains in the crystal structure generate an anisotropy in several physical properties [39]. Several literatures during the past addressed the stability of ReS₂ through phonon spectra from experiment and theory [10,40]. Here we have also confirmed the structural stability through phonon dispersion of ReS₂ using finite displacement method using VASP, in conjunction with Phonopy [41], and we find the spectra is in good agreement with the earlier reports.

The schematic crystal structure and phonon dispersion for ambient ReS₂ are given in Fig. 1. The compound has 12 atoms, which leads to 36 phonon modes. While focusing on the phonon dispersion, one can clearly see that the dispersion along different crystallographic directions are different. In base plane (along 'a' and 'b' directions) we have observed almost similar behaviour of acoustic phonon modes, and optical and acoustic phonon interactions are observed near 100 cm⁻¹, which might increase the scattering of phonons and suppresses the thermal conductivity [42]. Along 'c' axis the scenario is quite different, acoustic phonon modes are found to be little lesser dispersive and overlapping of acoustic and optical modes is almost nil. This difference

might cause an anisotropy in thermal conductivity. One of the recent study has reported the in-plane and through plane anisotropy of thermal conductivity and the in-plane value is found to be around 70 W m⁻¹K⁻¹, and through plane value is around 0.55 W m⁻¹K⁻¹ [43].

3.2. Electronic structure and thermoelectric properties of ReS₂ in both bulk and layered forms

Electronic structure of ReS₂ in bulk, monolayer and bilayer forms from our study are presented in Fig. 2(a,b,c). Several previous studies [10,44–48] investigated the nature of band gap in this compound, which are contradicting. Among them, few studies proposed indirect band gap of ReS₂ [48,44] from experiment. Very recent study by Echeverry and Gerber theoretically predicted direct band gap in ReS₂ using GW method, and our present study is in good agreement with the same [47]. We have observed a direct band gap nature for bulk ReS₂ with a band gap around 1.2 eV. The band dispersion along different crystallographic directions is found to be different. The overall band profile of ReS₂ is comparable with other celebrated transition metal dichalcogenides. In general TMDs are well known for high thermopower [49], and in this compound also, we can observe flat bands aligned in both valence and conduction bands, which might contribute to thermopower. Looking into the band structure it is quite clear that, both valence and conduction bands are dominated by Re-'d' states [50]. Compared to Re-'d' states, the contribution from the S('s','p') states are very less, even though there exist a strong hybridization between Re-'d' states and S-'p' states. The effective mass values in the unit of electron mass along different crystallographic directions, again projects the inherent anisotropy present in the system (see Table 2). Fig. 2(b) reveals the band structure for monolayer ReS₂, which is similar to bulk

Table 2Comparison of bulk/monolayer at ambient and strained state (16%) in ReS₂, m^* (unit of m_e), σ/τ (unit of $\Omega^{-1}m^{-1}s^{-1}$) and Power-factor (P.F in unit of $W/mK^2 s$).

ReS ₂	m^* (in-plane)	m^* (c-axis)	σ/τ (in-plane)	σ/τ (c-axis)	P.F(in-plane)	P.F (c-axis)
Bulk	1.92,1.5	2.18	2×10^{16}	2×10^{15}	8×10^9	3×10^9
Bulk(strain)	2.4, 4.24	38.3	1×10^{20} , 9.5×10^{19}	3×10^{18}	10×10^{11}	3×10^9
monolayer	1.9,1.6		2×10^{16}		8×10^9	
Monolayer(strain)	2.48, 3.32		1×10^{20}		10×10^{11}	

band structure with slightly higher band gap compared to bulk. The band gap of monolayer ReS₂ is observed around 1.42 eV. It is to be noted that in other TMDs band gap nature is found to be different from bulk to monolayer [51]. A close analysis of the band structures of bulk and monolayer form shows that, there is a slight change in the band dispersion along X and Y high symmetry points, these small layer dependent nature has been reported in the previous study also [47]. Now let us analyse the bilayer band structure (see Fig. 2(c)), which is also almost identical to bulk and monolayer, with a direct band gap of 1.36 eV. We would also like to mention here that this small layer dependence is not significantly reflected in the thermoelectric properties from our calculations.

Now we brief the transport properties of ReS₂ in both bulk and layered forms. Thermoelectric coefficients such as thermopower, electrical conductivity scaled by relaxation time (will be represented as electrical conductivity throughout the manuscript) and powerfactor are calculated for bulk, monolayer and bilayer form of ReS₂. Similar to the other TMDs, the thermopower value of ReS₂ is found to be appreciable, and the same for bulk, monolayer and bilayer forms are given in Fig. 2(d,e,f). For better understanding, the variation of thermopower, electrical conductivity and power-factor as a function of carrier concentration at different temperature are represented in S1 (see Supplementary Fig. 1). From the analysis, we find both holes and electron doping to be favourable for TE applications. Magnitude of thermopower is found to be decreased with increasing carrier concentration for both holes and electrons. Small anisotropy along different crystallographic directions are observed, in accordance with band dispersion anisotropy. For hole doping, the thermopower value along 'a' axis is found to be little higher than the other two, and for electron doping 'c' direction values are found to be slightly enhanced. Maximum thermopower for hole doping is found to be $600 \mu V K^{-1}$ and for electrons the same is found to be around $540 \mu V K^{-1}$, which is comparable with well-established MoSe₂ and WSe₂, where the 'S' value are found to be $590 \mu V K^{-1}$ and $580 \mu V K^{-1}$ respectively [52]. In the case of electrical conductivity, we can observe a significant anisotropy between the crystallographic directions, and basal plane values secured the maximum for both holes and electrons, which projects the inherent quasi two dimensional nature, and the magnitude of electrical conductivity for electrons is found to be more than holes. From the power-factor values, it is clearly seen that both holes and electrons are beneficial with electron possessing slightly higher value, and the range of power factor is not very far from well-established TMD TE materials. The thermoelectric coefficients are found to be promising for a wide range of temperature (see Fig. S1). We have computed the range of relaxation time with help of reported conductivity value of ReS₂, and the estimated relaxation time is found to be around 10^{-17} s, which is of the same order of WSe₂ [52].

Since electronic structure properties are same for both bulk and layered forms, we can expect the same to be reflected in transport properties also. Fig. 2(e,f) shows the thermopower of monolayer and bilayer, and the magnitude of thermopower is found to be little enhanced in monolayer (Fig. 2 (e)), than the bulk, but the trend is found to be the same for both monolayer and bilayer. In the case of electrical conductivity (see S2 (Fig. 2 in Supplementary)), we could see similar behaviour as bulk. Altogether the thermoelectric properties of bulk and layered forms are found to be similar, implying the layer independent transport properties of ReS₂. Further we were inquisitive

to improve the transport properties, and we have applied uni-axial compressive strain along 'a' on bulk and monolayer ReS₂. The upcoming section deals with the effect of uni-axial strain on electronic structure and TE properties.

3.3. Effect of uni-axial strain in bulk and monolayer form of ReS₂

As hinted earlier, a systematic analysis of electronic and TE properties are performed under the application of uni-axial compression strain along 'a' direction, which covers up to a wide range of 20% lattice variation. The percentage of uni-axial strain is defined as $((a - a_0)/a_0) \times 100$. The basic strain tensor for three dimensional system is

$$\begin{bmatrix} \epsilon(1) & \epsilon(12) & \epsilon(13) \\ \epsilon(21) & \epsilon(22) & \epsilon(23) \\ \epsilon(31) & \epsilon(32) & \epsilon(33) \end{bmatrix}$$

where $\epsilon(ii)$ are strain along i^{th} direction, and $\epsilon(ij)$ is shear strain.

One of the recent study on ReS₂ has revealed the pressure effects on the electronic structure resulting in metallization at high pressure around 70 GPa, and the same inspired us to investigate the effect of uni-axial strain on ReS₂. First let us analyse the case of bulk ReS₂. The band gap is found to decrease and the band gap nature is found to turn from direct to indirect as a function of compressive strain along 'a' direction (see Supplementary Fig. 3(b)). An appreciable amount of change is observed in band dispersion along different crystallographic directions as a function of a-axis compressive strain, which eventually is reflected in the anisotropic nature in transport properties. The band structure at different strained states are given in Supplementary (Fig. 3(a,b)). At around 5% strain, the compound is almost quasi two dimensional, where the $\Gamma - X$ and $\Gamma - Y$ band dispersions are very similar and along $\Gamma - Z$, we could see highly flat bands. For further strain around 10% the scenario is changed completely, where we could see a significant difference in band dispersion within the plane and between basal plane and 'c' axis. Around 16% strain the system metallizes and the band structures at 16% strained state together with ambient one are represented in Fig. 3(a). From the figure it is evident that apart from metallization the band profile of the compound is drastically changed. At strained state, the dispersion along $\Gamma - X$ is found to be very high compared to other two directions, which might induce a huge anisotropy in system resulting in dimensional reduction. The calculated effective mass along different crystallographic direction further provide the glimpse of two dimensionality of the system, where effective mass in the unit of 'electron mass' along $\Gamma - X$ and $\Gamma - Z$ are 1.92 and 2.18 respectively at ambient and for strained state it turns out to be 2.49 and 38.3 reflecting the flat bands along the $\Gamma - Z$ direction. At the metallized state, there are two bands which cross the Fermi level, and that corresponds to two Fermi surfaces, among which one is a hole like FS and another is an electron like FS (see Fig. 4(c)). These two surfaces are very thin sheets with different shapes. It is quite evident that the bands along $\Gamma - Y$ is found to be very flat, and indicate the two dimensional nature of the system. The stability of this strained state is further confirmed by phonon dispersion analysis, and the same is given in Fig. 3(c). A quick comparison with ambient state brings out the fact that, the phonon dispersion is found to be different at the strained state, the optical

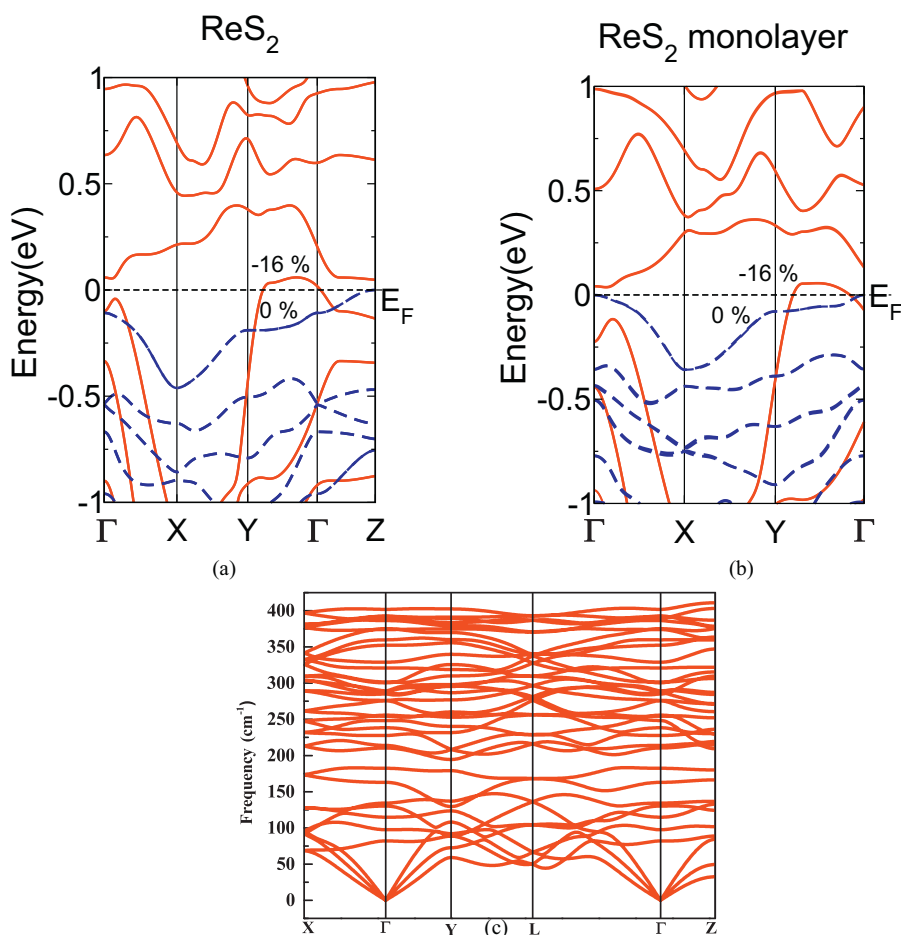


Fig. 3. Band structure of bulk and monolayer ReS₂ at different compressive strains, blue dashed lines represent the ambient state and red line represent the strained state a) bulk, b) monolayer, c) phonon dispersion for bulk ReS₂ at 16% strain. (For interpretation of the references to color in this figure legend, the reader is referred to the web version of this article.)

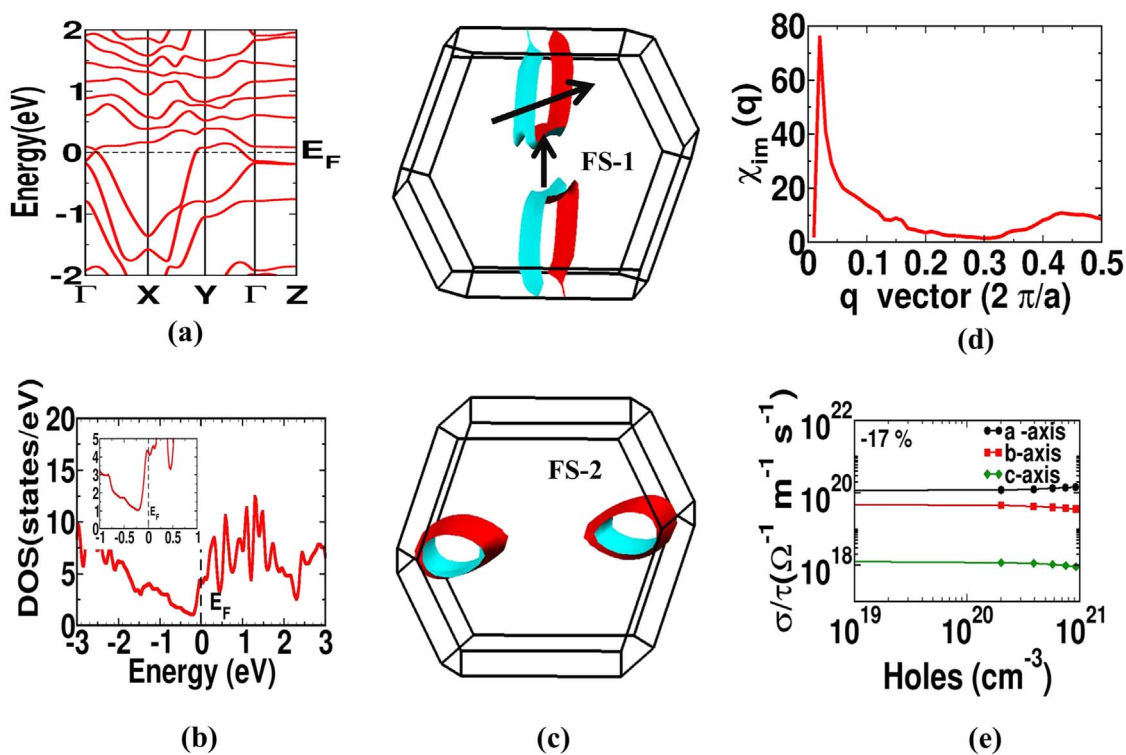


Fig. 4. Properties at 17% strain. a) band structure b) density of states, c) Fermi surface, d) imaginary part of susceptibility, e) electrical conductivity scaled by relaxation time.

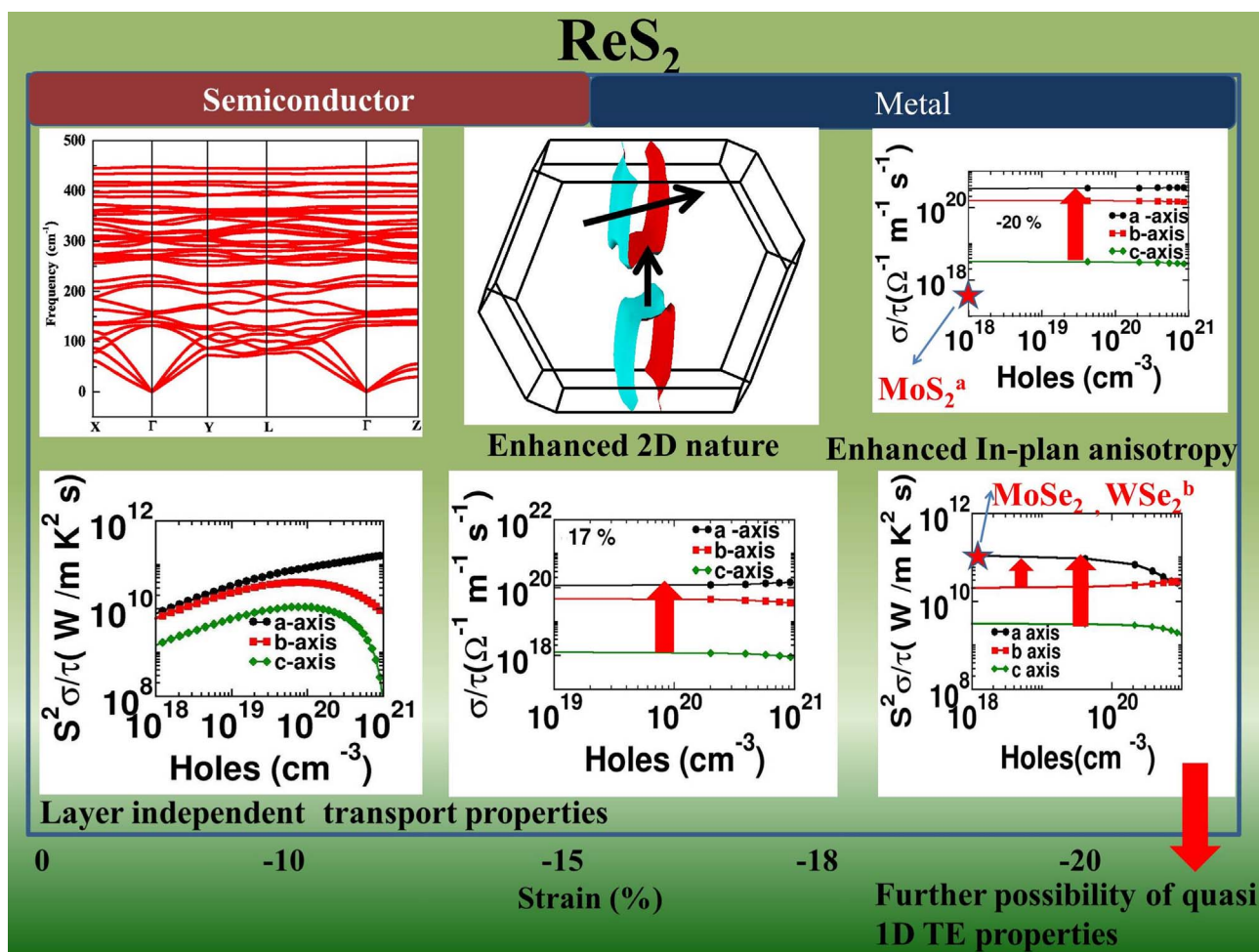


Fig. 5. Schematic of ReS₂, and comparison with other established compounds. a: Ref. [55], b: Ref. [52].

phonons are shifted to low frequency range along Γ - Z direction, which increases the possibility of interaction between acoustic and optical phonons, thereby one might expect a reduction in thermal conductivity value. For further strain around 17% we could observe more flat nature of bands and highly nested Fermi surface. The hole like FS is represented as FS-1 and electron like FS is named as FS-2 (see the Fig. 4(c)). From the Fermi surface plots, one can evidence the nesting of Fermi surface happening in two directions, as represented with arrow marks. To elucidate more about nesting of Fermi surface authentically, we have calculated the real and imaginary part of the generalised susceptibility $\chi(q)$, where q is the wave-vector of FS-1 along the high symmetric direction Γ - Y. The singularity observed in the imaginary part of the susceptibility gave a clear evidence of Fermi surface nesting (See Fig. 4(d)) along that direction. More prominent flat Fermi surface is observed in the second direction, and due to the lack of high symmetry points along that direction, we did not calculate the $\chi(q)$, but one can always expect higher amount of nesting towards that direction. In the previous study, the pressure induced structural transition (at around 90 GPa) and superconductivity in the transformed structure (around 102 GPa) was reported. Here, the observed peak in density of states (as shown in Fig. 4(b)) at Fermi level and highly nested Fermi surface are throwing light on the possibility of superconducting state and need to be verified [54]. Moreover the anisotropy in transport property like electrical conductivity gave further evidence for this two dimensional nature in strained bulk ReS₂. In addition, the response of uni-axial strain is examined in monolayer also, and we could see a very similar kind of metallization happening around 16% strain (see Fig. 3(b)), which again substantiate the dimensional reduction. A recent study has examined the stability of 'x'-axial

strained states using phonon dispersion [17], where they have claimed the stability to be vanish around 12%. It is to be noticed that the initial volume of the reported study is found to be lesser than our ambient volume for monolayer, and our 16% volume is well within their stability region, which ensure the dynamical stability of the strained state.

Interesting thermoelectric coefficients are found as a function of strain, and the anisotropic nature is more pronounced. The anisotropy in the band dispersion as a function of strain is reflected in the transport properties also. The power-factor at different strains are provided in Supplementary Fig. 3(c,d). At 5% strain we could see a quasi two dimensional nature, where basal plane properties are almost found to be same and enhanced compared to 'c' axis. Subsequently for 10% strain, almost one order difference in power factor is observed within the basal plane and between 'a' and 'c' axis the anisotropy has turned to 2 order. Concentrating on the metallized state (17%), the magnitude of thermopower is found to be reduced as expected due to metallization, and the vital point is, along 'a' direction the value of thermopower is found to be around $40 \mu\text{V K}^{-1}$ for hole doping and for the other two direction we could see the sign change because of carrier flipping. A compensating incremental nature is observed in electrical conductivity which again benefits for net thermoelectric performance. Higher value of electrical conductivity and moderate value of thermopower, result in promising value of power-factor in the basal plane, which is found to be higher than the ambient value at low carrier concentrations. The variation of electrical conductivity and power factor as a function of carrier concentration at 17% strained state is represented in S4 (Supplementary Fig. 4(a,b)). The in-plane power factor values are found to be two orders higher than the out of plane power factor, which again supports the two dimensional

characteristics of the strained state [53]. A similar in-plane electrical conductivity values are observed for monolayer also, which is represented in Supplementary Fig. 4(c). Moreover the phonon dispersion at the strained state is found to be promising, where the interaction between the acoustic and optical phonons are found to be in low frequency range around 60 cm^{-1} , which might result in low values for thermal conductivity in this state. In general the semiconducting states are considered to be more promising for thermoelectric application, but here, we could find a higher value of power factor in the metallized state. At metallization in this strained state, the band dispersions along $\Gamma - X$, $\Gamma - Y$ and $\Gamma - Z$ are anisotropic, which lead to an asymmetry in density of states as seen in Fig. 4(b), which further emphasises the fact that holes are more favourable carriers in ReS_2 . While focusing on the power factor plot, one can clearly observe that there is a small in-plane anisotropy in the strained state. For further strain around 20% we could see more than one order difference between the power factor along 'a' and 'b' axis, and two order difference between 'a' and 'c' axis (included in Fig. 5). The developed enormous in-plane anisotropy indicates the possibility of using ReS_2 nanowires for TE applications, which has to be taken as future project. Sequence of calculations have provided the clear picture of metallization, increasing anisotropy and an enhancement in power-factor along 'a' direction in the system as an effect of uni-axial strain, and ReS_2 has turned to be an excellent candidate for diverse fields like thermoelectrics, straintronics applications etc. In Table 2 we have represented the effective mass, electrical conductivity and power factor for ambient and strained state of bulk and monolayer, which clearly shows the enhanced anisotropy as a function of strain. Moreover, Fig. 5 represents the schematic of our overall study together with the comparison of other TMD, and summarize the semi-conductor to metal transition in ReS_2 . As a function of strain, the electrical conductivity is found to be enhanced, and the phonon dispersion analysis has further provided the clue for reduction of thermal conductivity. This shows the possibility of better thermoelectric performance in the strained state. In addition, a similar kind of metallization is observed in the monolayer which further shows promising dimensional reduction with enhanced electrical conductivity, which certainly projects ReS_2 to be more versatile TMD compared to others. If one can improve the thermopower value, without suppressing the conductivity value, ReS_2 might turn to be a promising candidate for nanowire TE applications.

4. Conclusions

Semiconductor-metal transition together with enhanced 2D nature is predicted in ReS_2 under the application of uni-axial strain in bulk ReS_2 . In line with bulk, monolayer ReS_2 also emerges to be a metal at strained state (around 16%), further emphasising the layer independent properties of ReS_2 . The anisotropic property in the strained monolayer opens up the possibility of further dimensional reduction in the system which need to be inspected. In addition to that the thermoelectric properties are also analysed, and are found to be promising in ReS_2 for both bulk and layered forms. Our results indicate the possibility of using ReS_2 as a TE material in different forms.

Acknowledgement

The authors SPC and VK would like to thank IIT Hyderabad for computational facility, and SPC would like to thank MHRD for fellowship. The author GV would like to thank DRDO through ACRHEM for the financial support under the grant no DRDO/18/1801/2016/01038: ACRHEM - PHASE - 111.

Appendix A. Supplementary data

Supplementary data associated with this article can be found in the online version at <http://dx.doi.org/10.1016/j.jssc.2018.09.008>.

References

- [1] S. Manzeli, D. Ovchinnikov, D. Pasquier, O.V. Yazyev, A. Kis, *Nat. Rev. Mater.* 2 (2017) 17033.
- [2] N. Kumar, J. He, D. He, Y. Wang, H. Zhao, *J. Appl. Phys.* 113 (2013) 133702.
- [3] B. Wang, Y. Liu, K. Ishigaki, K. Matsubayashi, J. Cheng, W. Lu, Y. Sun, Y. Uwatoko, *Phys. Rev. B* 95 (2017) 220501 (R).
- [4] Q.H. Wang, K. Kalantar-Zadeh, A. Kis, J.N. Coleman, M.S. Strano, *Nat. Nanotechnol.* 7 (2012) 699.
- [5] Z. Lin, B.R. Carvalho, E. Kahn, R. Lv, R. Rao, H. Terrones, M.A. Pimenta, M. Terrones, *2D Mater.* 3 (2016) 022002.
- [6] Aleksander A. Tedstone, David J. Lewis, Paul O'Brien, *Chem. Mater.* 28 (2016) 1965.
- [7] Q.H. Wang, et al., *Nat. Technol.* 17 (2012) 699.
- [8] A. Kumar, P.K. Ahluwalia, *Eur. Phys. J. B* 85 (2012) 186.
- [9] D.E. Bugaris, C.D. Malliakas, D.P. Shoemaker, Dat T. Do, D.Y. Chung, S.D. Mahanti, M.G. Kanatzidis, *Inorg. Chem.* 53 (2014) 9959.
- [10] S. Tongay, et al., *Nat. Commun.* 5 (2014) 3252.
- [11] Zhao Zhao, et al., *Nat. Commun.* 6 (2015) 7312.
- [12] S. Song, et al., *Nano Lett.* 16 (2016) 188.
- [13] X. Wang, *Sci. Rep.* 7 (2017) 46694.
- [14] K. Friemelt, et al., *J. Appl. Phys.* 74 (1993) 5266.
- [15] E. Zhang, et al., *Adv. Funct. Mater.* 25 (2015) 4076.
- [16] Chris M. Corbet, et al., *ACS Nano* 9 (2015) 363.
- [17] Yan-ling Li, et al., *Int. J. Hydrog. Energy* 42 (2017) 161.
- [18] Y.M. Min, *Appl. Surf. Sci.* 427 (2018) 942.
- [19] Wen Wen, *small*, 2017, 1603788.
- [20] D.A. Chenet, et al., *Nano Lett.* 15 (2015) 5667.
- [21] Yung-Chang Lin, et al., *ACS Nano* 9 (2015) 11249.
- [22] Dawei Zhou, et al., *Quantum Mater.* 2 (2017) 19 (npj).
- [23] S. Bhattacharyya, Tribhuwan Pandey, Abhishek K. Singh, *Nanotechnology* 25 (2015) 465701.
- [24] G. Kresse, J. Furthmuller, *Phys. Rev. B* 54 (1996) 11169.
- [25] G. Kresse, J. Furthmuller, *Comput. Mater. Sci.* 6 (1996) 15.
- [26] A. Tkatchenko, R.A. Di Stasio, R. Car, M. Scheffler, *Phys. Rev. Lett.* 108 (2012) 236402.
- [27] P. Blaha, K. Schwarz, G.K.H. Madsen, D. Kvasnicka, J. Luitz, WIEN2k: an augmented plane wave +localorbitals program for calculating crystal properties, Techn. Universitat Wien, Austria, 2001 (Karlheinz Schwarz).
- [28] P. Blaha, K. Schwarz, P.I. Sorantin, S.B. Tricky, *Comput. Phys. Commun.* 59 (1990) 399.
- [29] G.K.H. Madsen, D.J. Singh, *Comput. Phys. Commun.* 67 (2005) 175.
- [30] T.J. Scheidmantel, C. Ambrosch-Draxl, T. Thonhauser, J.V. Badding, J.O. Sofo, *Phys. Rev. B* 68 (2003) 125210.
- [31] L. Jodin, J. Tobola, P.P. Echeur, H. Scherrer, S. Kaprzyk, *Phys. Rev. B* 70 (2004) 184207.
- [32] L. Chaput, P. Pecheur, J. Tobola, H. Scherrer, *Phys. Rev. B* 72 (2005) 085126.
- [33] K.P. Ong, D.J. Singh, P. Wu, *Phys. Rev. B* 83 (2011) 115110.
- [34] D.J. Singh, I.I. Mazin, *Phys. Rev. B* 56 (1997) R1650.
- [35] D. Parker, D.J. Singh, *Phys. Rev. B* 82 (2010) 035204.
- [36] G.K.H. Madsen, K. Schwarz, P. Blaha, D.J. Singh, *Phys. Rev. B* 68 (2003) 125212.
- [37] L. Zhang, M.-H. Du, D.J. Singh, *Phys. Rev. B* 81 (2010) 075117.
- [38] C.H. Ho, Y.S. Huang, K.K. Tiong, P.C. Liao, *J. Phys: Condens. Mater.* 11 (1999) 5367.
- [39] C.H. Ho, Y.S. Huang, J.L. Chen, T.E. Dann, K.K. Tiong, *Phys. Rev. B* 60 (1999) 766.
- [40] Rui He, Jia-An Yan, Zongyou Yin, Zhipeng Ye, Gaihua Ye, Jason Cheng, Ju Li, C.H. Lui, *Nano Lett.* 16 (2016) 1404.
- [41] A. Togo, Isao Tanaka, *Scr. Mater.* 108 (2015) 1.
- [42] J. Ding, Ben Xu, Yuanhua Lin, Cewen Nan, Wei Liu, *New J. Phys.* 17 (2015) 083012.
- [43] H. Jang, Christopher R. Ryder, Joshua D. Wood, Mark C. Hersam, David G. Cahill, *Adv. Mater.* 650 (2017) 1700.
- [44] Ozgur Burak Aslan, Daniel A. Chenet, Arend M. van der Zande, James C. Hone, Tony F. Heinz, *ACS Photonics* 3 (2016) 96.
- [45] D. Biswas, Alex M. Ganose, R. Yano, J.M. Riley, L. Bawden, O.J. Clark, J. Feng, L. Collins-Mcintyre, M.T. Sajjad, W. Meevasana, T.K. Kim, M. Hoesch, J.E. Rault, T. Sasagawa, David O. Scanlon, P.D.C. King, *Phys. Rev. B* 96 (2017) 085205.
- [46] James L. Webb, Lewis S. Hart, Daniel Wolverson, Chaoyu Chen, Jose Avila, Maria C. Asensio, *Phys. Rev. B* 96 (2017) 115205.
- [47] J.P. Echeverry, I.C. Gerber, *Phys. Rev. B* 97 (2018) 075123.
- [48] Ignacio Gutiérrez-Lezama, Bojja Aditya Reddy, Nicolas Ubrig, Alberto F. Morpurgo, *2D Mater.* 3 (2016) 045016.
- [49] C. Lee, Jisook Hong, Myung-Hwan Whangbo, Ji Hoon Shim, *Chem. Mater.* 25 (2013) 3745.
- [50] A. Splendiani, L. Sun, Y. Zhang, T. Li, J. Kim, Chi-Yung Chim, G. Galli, Feng Wang, *Nano. Lett.* 10 (2010).
- [51] ason K. Ellis, Melissa J. Lucero, Gustavo E. Scuseria, *Appl. Phys. Lett.* 99 (2011) 261908.
- [52] S. Kumar, U. Schwingenschlo, *Chem. Mater.* 27 (2015) 1278.
- [53] V.K. Gudelli, V. Kanchana, G. Vaitheeswaran, D.J. Singh, A. Svane, N.E. Christensen, Subhendra D. Mahanti, *Phys. Rev. B* 92 (2015) 045206.
- [54] S. Chandra, S. Mathi Jaya, M.C. Valsakumar, *Phys. C* 432 (2005) 116.
- [55] G. Huai-Hong, Yang Teng, Tao Peng, Zhang Zhi-Dong, *Chin. Phys. B* 23 (2014) 017201.
- [56] H.H. Murray, et al., *Inorg. Chem.* 33 (1994) 4418.